

Correlation Between AC Core Loss and Surface Magnetic Barkhausen Noise in Electric Motor Steel

Arash A. Samimi · Thomas W. Krause · Lynann Clapham ·
Matthew Gallagher · Yaoyao Ding · Pampa Ghosh ·
Richard Chromik · Andrew M. Knight

Received: 25 June 2014 / Accepted: 30 August 2014 / Published online: 16 September 2014
© The Author(s) 2014. This article is published with open access at Springerlink.com

Abstract Core loss is a significant source of energy loss in electric motor steel laminates. Therefore, there is interest in monitoring the quality and consistency of laminates at various stages of manufacturing. The purpose of this study was to investigate the feasibility of using surface magnetic Barkhausen noise for the evaluation of AC core loss, and further, to examine potential origins of magnetic loss in non-oriented electrical steel. Core loss values were measured by a single sheet tester and Barkhausen noise measurements were performed using pole flux control on eight laminates with various grain size, texture and composition. Magnetocrystalline energy was calculated from X-ray diffraction data to quantify texture. Results demonstrated higher surface Barkhausen emissions for samples with lower core loss. Barkhausen noise analyses were used to examine the interplay among core loss, grain size, magnetocrystalline energy and B–H characteristics. The inverse correlation between core loss and Barkhausen noise emissions was qualitatively explained in terms of the orthogonal vector contribution of microscopic eddy currents to losses associated with bulk currents arising in the sample during magnetization.

Keywords Barkhausen noise · Flux control · Magnetic non-destructive testing · Core loss · Electrical steel

1 Introduction

This work reports the results from a collaborative study on the correlation between core loss and Barkhausen noise in non-oriented electrical steel (NOES) laminates, with applications to electric motors. The motivation of this work is the development of magnetic Barkhausen noise (MBN) as a non-destructive means of identifying factors that may affect core loss in NOES, which is of interest to an industrial partner. Furthermore, this work contributes to a better understanding of magnetic loss mechanisms, which can lead to improvement in the production of energy efficient laminates.

NOES or non-oriented Silicon–Iron steel is the most widely used soft ferromagnetic material, with applications in rotary machines [1]. Among the significant properties of NOES laminates are high permeability, low magnetic loss and low magnetostriction, which is achieved by an optimum combination of various factors including texture, grain size, composition and thickness [2,3]. The demand for energy efficiency in electric motors and rotary machines has driven the growth of NOES in the world market, with the characterization of magnetic loss as the main target in NOES research [4]. Nevertheless, loss measurement and its evaluation is limited by: (1) Deficiencies in the traditional loss measurement techniques, i.e. the Epstein square or a single sheet tester. These are destructive, off-line and typically provide only an average of the magnetic properties in the rolling or transverse direction [5–8]. Therefore, development of a nondestructive evaluation technology could provide benefits for condition monitoring at various stages of manufacture. (2) The understanding of the Epstein technique is also

A. A. Samimi (✉) · L. Clapham
Applied Magnetism Group, Queen's University, Kingston,
ON K7L 3N6, Canada
e-mail: arashie80@gmail.com

T. W. Krause
NDE Development, Royal Military College of Canada, Kingston,
ON K7K 7B4, Canada

M. Gallagher · Y. Ding · P. Ghosh · R. Chromik
Department of Mining and Materials Engineering,
McGill University, Montreal, QC H3A 0C5, Canada

A. M. Knight
Department of Electrical and computer Engineering,
University of Alberta, Edmonton, AB T6G2V4, Canada

limited by the absence of a 3-D model, which properly incorporates domain wall dynamics into total loss calculations [1]. Furthermore, a standard approach is to express total loss as the sum of hysteresis, bulk eddy current and an excess term, which compensates for the observed total loss [1,9]. However, this approach ignores the influence of domain wall dynamics on magnetization processes and loss mechanisms [1,10,11]. Information about domain wall processes can be obtained from MBN emissions [12], which may be incorporated into a physical model to improve loss calculations. Therefore, MBN may provide the “missing link” in magnetic loss characterization.

MBN reflects clustering of magnetization discontinuities, which are temporally and spatially correlated jumps of domain walls [12–15]. The Barkhausen noise spectrum is affected by material microstructure [16,17], texture [18], magnetic easy axis direction in which domain magnetization vectors tend to align [19], and stress state of the material [20], which in turn influence the magnetic loss. Therefore, it is expected that Barkhausen emissions contain information about the magnetic loss within ferromagnetic laminates [1]. The generation of Barkhausen noise is influenced by domain nucleation and annihilation processes, which typically occur at grain boundaries [11,14]. The average time duration of a clustered pulse of Barkhausen emission is directly proportional to grain size [14], which also correlates with the magnetic loss. Domain wall motion is accompanied by localized eddy currents (micro-eddy currents) [10]. The resulting inhomogeneous distribution in permeability due to micro-eddy currents is related to higher losses in silicon iron steels [21].

The correlation between MBN and core loss in grain oriented electrical steel laminates has been investigated in a limited number of earlier papers where the MBN technique is applied under field or current control [22–24]. The present work uses a flux-controlled MBN technique to further investigate the applicability of MBN for non-destructive monitoring of core loss in NOES. Flux control has been achieved by using pole feedback control of magnetic flux waveforms, to improve MBN reproducibility. An in-house designed and built flux controller combines an analog circuit with a digital algorithm for rapid surface measurements with minimum error in the control loop [25]. Control of flux reduces the likelihood of potential artifact effects such as those introduced by air gaps, and increases the reproducibility of measurement results [25–27].

2 Materials and Methods

2.1 Samples

The samples were eight semi-processed and fully-processed NOES laminates having standard widths of 30 mm. An

Table 1 Measured parameters for non-oriented electrical steel laminates with increasing ac core loss (W) at 1 T at 30 Hz

Sample #	D (μm)	T (mm)	W (W/kg)	μ_r	H_c (A/m)	B_R (T)
1	198	0.35	0.3223	13141.42	23.78	0.7468
2	177	0.35	0.3178	15604.88	24.03	0.7885
3	186	0.35	0.3151	15233.12	23.47	0.7552
4	167	0.35	0.3083	16410.95	23.05	0.7857
5	129	0.30	0.3031	17703.06	22.10	0.8178
6	130	0.30	0.2976	17081.01	21.99	0.8049
7	128	0.25	0.2871	19654.62	20.92	0.8389
8	123	0.25	0.2861	19293.19	20.99	0.8364

D (grain diameter), T (thickness), μ_r (permeability), H_c (coercivity), B_R (remanence)

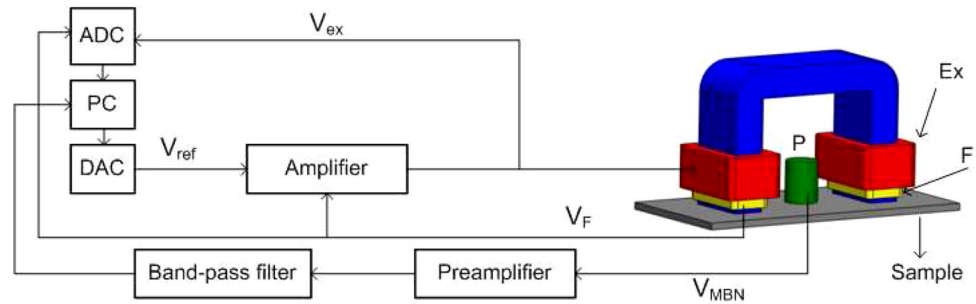
insulating coating with a measured thickness of 1 μm was uniformly distributed over the laminate surface.

2.2 Magnetic Measurements

Bulk magnetic characteristics and core loss in the samples were measured along the rolling direction (RD) under ac excitation at 1 T flux density at 30 Hz using a single sheet tester. These measurements were performed at University of Alberta. The samples had associated core loss values (W) as listed in Table 1, along with sample thickness (T), grain diameter (D) and measured B–H parameters.

Local magnetic measurements were performed using a flux-controlled Barkhausen noise system at Queen’s University. The MBN apparatus consisted of a surface dual-core probe (tetrapole) [25,28] in combination with an in-house designed magnetic flux controller, which controlled the flux waveform to obtain consistency and repeatability in local MBN measurements [25,26]. Figure 1 is a schematic diagram of one of the flux-controlled cores of the tetrapole probe. The poles of the U-shaped Supermendur core had cross sections of 4.2 mm × 9.5 mm and were 21.2 mm apart. Each pole was wrapped with a 500 turn excitation coil and a 50 turn feedback coil, which monitors the flux at the closest distance to the sample surface. As shown in the schematic in Fig. 1, a reference voltage, V_{ref} is generated by a digital-to-analog converter and fed into an analog feedback amplifier. The excitation coil voltage, V_{ex} , and the measured feedback coil voltage, V_F , are sampled by an analog-to-digital converter and processed through a personal computer. V_{ref} is adjusted in each iteration and the control loop repeats until V_F converges to the target feedback coil voltage. The convergence time (time to measure) is less than 10 s for frequencies between 10 to 100 Hz, which are typically used in NDT measurements [25]. The tetrapole probe uses flux superposition to achieve a net magnetization in the plane of the laminate

Fig. 1 Schematic diagram of the flux-controlled MBN system showing the feedback loop and the probe with the excitation (Ex), feedback (F) and peak-up (P) coil



in different orientations. This permitted angular Barkhausen measurements on two of the samples characterized by the highest and lowest core loss values, respectively.

A spring-loaded solenoidal pick-up assembly, shown in green in the center of the pole pieces in Fig. 1, used a ferrite core, which is wrapped with 100 turns of AWG 44 copper coil, surrounded by a permeable sheath and assembled into a conductive brass shield to minimize the sensing radius to about 2.4 mm at 30 Hz [28]. Between the electromagnet poles, immediately beneath the small pick-up coil, finite element modeling has shown that the flux is uniform [28]. The high spatial resolution pick-up coil couples to the vertical magnetization components projected out of the surface of the sample, which in turn induce a voltage in the pick-up coil. The high frequency Barkhausen emissions (>1 kHz) were fed to a preamplifier and the low frequency excitation signal was filtered out. The rms envelope of the Barkhausen signal is produced and the total Barkhausen noise energy (BN_E) is then calculated as:

$$BN_E = \int (BN_{env})^2 d\phi, \tag{1}$$

in which ϕ is the feedback signal phase corresponding to time within the cycle. Similar to the single sheet B–H measurements, the flux-controlled MBN measurements were also taken at 30 Hz excitation frequency. This was the lowest frequency with which the current system could still maintain flux control. The peak flux density used for MBN measurements was 100 mT measured at the excitation magnet poles, which results in approximately four to five times higher flux density level within the laminates, taking into account the effect of sample thickness.

2.3 Grain Size and Texture Measurements

Preparation for texture and grain size measurements involved coating removal, polishing with 1 μ m oil-based diamond suspension and 3 % Nital etching to reveal the grain structure. Images were captured at 50 \times magnification using a Nikon Epiphot 200 optical microscope equipped with Clemex Image Analysis software. The grain size measurements were performed according to ASTM E112 [29].

Table 2 Chemical composition in wt%, and calculated magnetocrystalline energy (E_a) along RD

Sample #	Si	Al	E_a (J/m ³)
1	3.27	0.54	0.411
2	2.81	0.26	0.402
3	3.26	0.53	0.405
4	2.78	0.25	0.402
5	3.51	0.62	0.361
6	3.19	0.58	0.344
7	3.61	0.57	0.301
8	3.24	0.60	0.293

The chemistry was found using ICP-AES and combustion techniques

Texture measurements were performed at McGill University using X-ray diffraction on the top surface (rolling plane) of the samples. A Bruker X-Ray Diffraction Goniometer operating at 35 kV and 45 mA was used to capture diffraction data over a 6 mm \times 6 mm scanned area. Three incomplete pole figures [(110), (200), and (211)] were collected, and used to calculate the orientation distribution function (ODF) using TexTools software. To quantitatively correlate magnetic properties with texture, the ODF was then used to calculate the magnetocrystalline anisotropy energy (E_a) [30], i.e. the energy required to magnetize the sample along the RD. In addition to the texture information, the calculation for E_a incorporated the aluminum and silicon content. Table 2 includes the Al and Si contents, which were obtained from the ICP-AES analysis and combustion techniques, as well as the calculated value of E_a obtained using the first order anisotropy constant K_1 [30]:

$$K_1 = 4.77 - (0.21256)(\text{wt\%Si}) - (0.03816)(\text{wt\%Al}). \tag{2}$$

3 Results

3.1 Correlations with Core Loss

Figure 2 indicates an inverse relationship between core loss and MBN energy measured along the RD. This correlation implies that the optimum magnetic performance is achieved

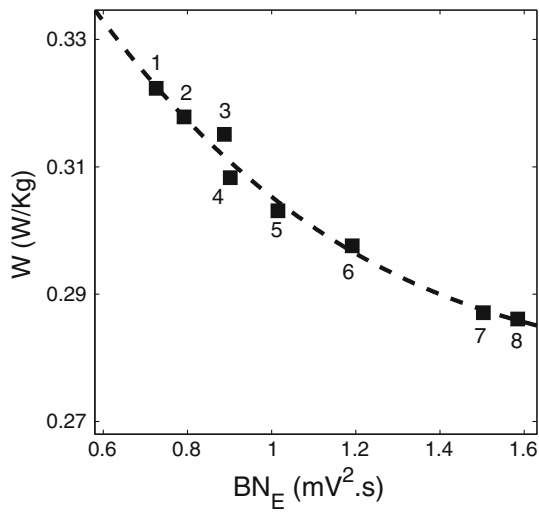


Fig. 2 The core loss as a function of Barkhausen energy (BN_E) along RD. The dotted line is the best polynomial fit to the data

when higher MBN emissions are measured, which is qualitatively in agreement with earlier studies [22,23] on grain oriented Si-Fe laminates. The most recent paper [24] also observed a strong correlation between MBN and core loss in both oriented and non-oriented Si-Fe laminates, however in that case the correlation was a direct, rather than an inverse one. The difference in behaviour from the present study is likely due to a smaller grain size relative to the previous samples [24] and a different level of excitation field. Figure 2 also demonstrates the relatively high sensitivity of the MBN technique to only a small range of variation in core loss.

3.2 Correlations with Grain Size and Texture

Figure 3 suggests a linear relationship between core loss and the inverse square root of grain diameter. This result agrees

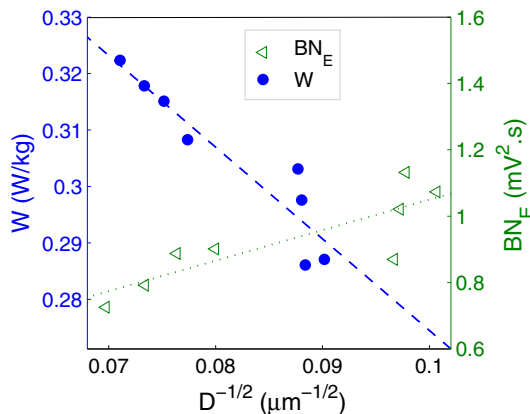


Fig. 3 Barkhausen energy (BN_E) and core loss (W) as a function of the inverse square root of the grain diameter (D)

with earlier observations for laminates with grains larger than the optimum size at which the lowest loss and highest permeability is achieved [2,3]. The observed inverse relationship between Barkhausen energy and grain size, agrees with the Hall-Petch relationship as given by [31]:

$$BN_E = C_g \cdot d_g^{-1/2}, \tag{3}$$

in which C_g is a constant and d_g is the grain size. The correlation R-squared factor associated with the observed Hall-Petch relationship is 0.71, which is statistically significant.

In fine grained steels, each grain surrounds a region of highly correlated 180° domain walls, known as magnetic objects [11]. The primary energy barrier, which defines the region of a magnetic object is, therefore, the grain boundary, at which nucleation and pinning of domain walls occur. As grain size increases, the grain boundary density per unit volume decreases [17] and Barkhausen energy is reduced according to a Hall-Petch relation for ferrite grains. As mentioned in Sect. 2.2, the thickness variations can result in approximately 25 % increase in sample flux density from the largest to the smallest laminate thickness, which in turn modifies the MBN generation. Therefore, in Fig. 3, Barkhausen energy was normalized to thickness, as performed elsewhere [23], to compensate for the thickness variations, and hence to more clearly examine the relationship of grain size with BN_E . To normalize MBN energy values, a dimensionless factor was introduced by normalizing the laminate thicknesses with respect to the largest thickness of 0.35 mm. The MBN energy values were then multiplied by this factor. The remaining scatter in the data may be due to the very small window of variations in other microstructural features of the laminates, which affect their magnetic properties.

Figure 4 plots linear correlations between core loss (W) and Barkhausen energy (BN_E) versus the magnetocrystalline

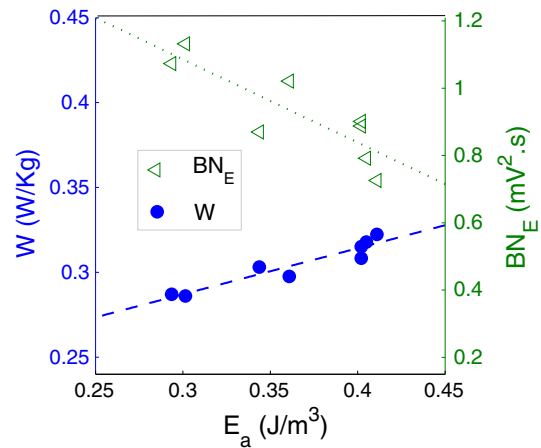
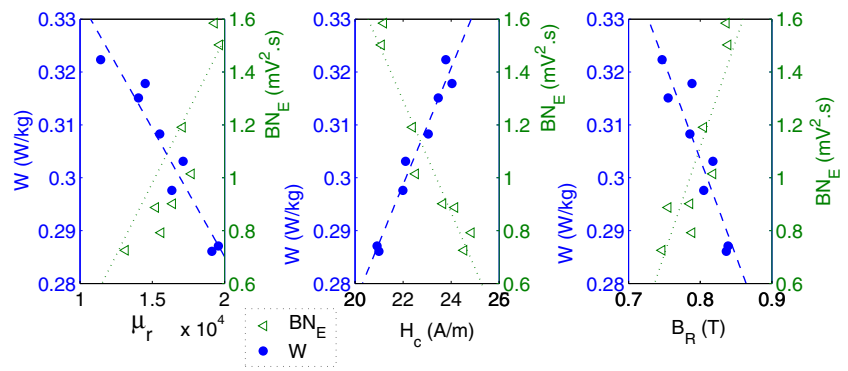


Fig. 4 Barkhausen energy (BN_E) and core loss (W) as a function of magnetocrystalline energy (E_a) along RD

Fig. 5 Correlations between Barkhausen energy (BN_E) and core loss (W) with hysteresis parameters, i.e. permeability (μ), coercivity (H_c) and remanence (B_R)



energy (E_a) determined along the RD. In this plot E_a and BN_E were both normalized to compensate for thickness variations. Lower E_a is associated with more magnetic easy axes aligned close to the RD, i.e. the energetically favorable direction of magnetization, and therefore, a higher MBN energy [32]. Furthermore, less energy is required to magnetize the samples with lower E_a , which in turn reduces the core loss [33,34] as observed in Fig. 4.

3.3 Correlations with B–H Characteristics

The variations in grain size and texture of the Si–Fe laminates modify the configuration of domain walls within the samples, which in turn influence the magnetic characteristics of the B–H loop, the core loss and the generation of Barkhausen noise. Figure 5 shows the interplay among these parameters. The variation of core loss with these three parameters, as shown in Fig. 5, is qualitatively in agreement with earlier observations for laminates with grains larger than the optimum size [2,3].

4 Discussion

This work investigated the interplay and correlations among MBN emissions, core loss, grain size, texture and B–H characteristics of the NOES laminates. The significant aspect of this work is the inverse correlation between Barkhausen energy and core loss, as shown in Fig. 2. In the following discussion, this correlation is interpreted in terms of the localized nonuniform magnetization changes within the ferromagnetic laminates as a result of abrupt domain wall motion.

The observation of correlations between Barkhausen noise energy and core loss at 30 Hz suggests that the same parameters are present in both effects. These parameters are most likely associated with the influence of anisotropy energy on domain configuration and by extension the anisotropic Barkhausen noise energy as observed in Fig. 4. Therefore, the precise frequency is not a factor, but the particular domain interactions are. Reference [22], for example, correlates MBN and core loss at totally different magnetization

frequencies of 12 and 60 Hz, respectively. Furthermore, at higher frequencies, macroscopic eddy current effects make a progressively larger contribution, substantially complicating the magnetization in the sample.

The discontinuous movement of domain walls is accompanied by local micro-eddy currents, which are known to be a source of magnetic loss in ferromagnetic materials along with macroscopic eddy currents and hysteresis loss [10]. Micro-eddy currents circulate around the moving domain wall to oppose the local changes in magnetization, and thereby damp the velocity of domain walls and generate resistive heating [10,21]. Localized microscopic eddy currents add vectorily to bulk eddy current components to contribute to the total power loss (P) over the unit volume of the laminate sample given as [18,22,35]:

$$P = \rho \int (\bar{I}_{ma} + \bar{I}_{mi})^2 dv, \tag{4}$$

in which ρ is the resistivity of the material, \bar{I}_{mi} is the micro-eddy current vector associated with domain wall movements, and \bar{I}_{ma} is the homogeneous macroscopic eddy current component. Equation (4) indicates that the power loss is smaller for samples in which a larger amount of their micro-eddy current vector (\bar{I}_{mi}) is projected out of the surface of the laminate, with a consequently larger voltage induced into the surface Barkhausen pick-up coil [22]. Therefore, samples with lower loss exhibit larger Barkhausen energy as shown in Fig. 2.

An array of simultaneously moving (jumping) domain walls interacts with each other, and thereby cancels out their adjacent micro-eddy currents [10], which further reduces the total power loss [22]. It is therefore expected that a higher degree of micro-eddy current cancellation can further reduce the magnetic loss. To investigate this, Ref. [22] introduced a phenomenological parameter, α' , which indicates the strength of the eddy current field interactions between simultaneously moving domain walls that contribute to the magnetic easy axis of the laminate. α' is found by fitting an energy expression (E) to the angular Barkhausen measurements and is given by [22]:

$$E = \alpha \cos^2(\theta - \phi) + \alpha' \cos(\theta - \phi) + \beta, \quad (5)$$

in which θ is the angle of the field with respect to the sample magnetic easy axis, ϕ is the angle of the magnetic easy axis with respect to the RD. β is the isotropic background contribution to Barkhausen energy and is associated with the domain walls oriented randomly with respect to the magnetic easy axis. α and α' are fitting parameters associated with angular variations of MBN signal. The parameter of interest is α' , which is directly proportional to the local eddy current field interaction (H_{E_i}) given by the sum over the m th neighboring domain wall as [36]:

$$H_{E_i} = C_i \sum_m v_m e^{-X_{im}\pi/d}, \quad (6)$$

where C_i is a constant, v_m is the wall velocity, X_{im} is the distance between adjacent domain walls and d is the laminate thickness. Equation (6) indicates that the micro-eddy current interaction is proportional to wall velocity (v), and exponentially decreases with the distance between the two adjacent walls. An increase in α' with decreasing power loss was observed in grain-oriented silicon laminates [22]. This was attributed to a finer spacing of 180° domain walls in samples with lower loss, which increases the interactions between micro-eddy currents by decreasing the distance between adjacent walls according to Eq. (6) [36]. The increase in micro-eddy current interactions, therefore results in a reduction in the contribution of micro-eddy currents to the loss process.

Following the same approach as Ref. [22], angular Barkhausen measurements were taken, as indicated in Sect. 2.2, on two of the samples under study with the lowest and highest core loss values, i.e. sample 8 and 1, respectively. Then the energy variations were plotted with respect to the angle of excitation as a polar plot shown in Fig. 6. The energy expression from Eq. (5) was used to calculate the α' values for sample 8 and 1, which were found to be 0.05 and 0.03 ($\text{mV}^2 \cdot \text{s}$) respectively, when taking into account the laminate thickness. A larger interaction parameter for the sample

with the lowest core loss, i.e. sample 8, is in agreement with Ref. [22].

Figure 6 also demonstrates a more pronounced magnetic anisotropy for sample 8 with the higher loss. A dimensionless anisotropy parameter, κ , was introduced to evaluate the degree of angular variations as [32]:

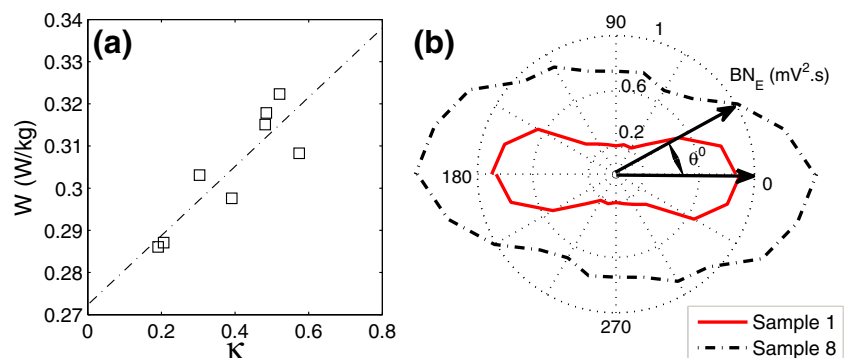
$$\kappa = \frac{BN_E(R) - BN_E(T)}{BN_E(R) + BN_E(T)}, \quad (7)$$

in which R and T corresponds to rolling and transverse direction respectively. Figure 6 shows an increase in core loss with increasing magnetic anisotropy, κ , which is attributed to a more inhomogeneous magnetization process [23]. Therefore, the smaller anisotropy and larger interaction parameter of sample 8 was correlated with its lower core loss relative to sample 1. Furthermore, the constantly higher Barkhausen noise energy of sample 8, as shown in Fig. 6, was attributed to its smaller grain size.

5 Conclusion

The present work investigated the applicability of surface Barkhausen noise measurements as a complementary, non-destructive method to the standard techniques for loss evaluation in NOES laminates. An in-house designed and built flux controller was used to effectively control the flux waveforms for local repeatable measurements at the surface of the laminates. A strong correlation was found between Barkhausen emissions and core loss for uni-directional magnetization applied along the RD. This correlation was established despite the very small variations in core loss values. The results were qualitatively explained in terms of micro-eddy currents, with higher interactions and therefore cancellation, likely for the samples having lower core losses. MBN was further correlated with grain size, texture and B–H curve parameters, which influence the core loss in the laminates. The angular MBN measurements showed that MBN may be used for local non-destructive evaluation of the magnetic anisotropy and magnetic easy axis, which influences the core

Fig. 6 **a** Core loss (W) as a function of the magnetic anisotropy factor (κ), **b** comparison of the angular Barkhausen measurements between samples with the highest and lowest core loss values, i.e. sample # 8 and #1 respectively



loss in the laminates. The results suggest that flux-controlled MBN has the potential to be a valuable inspection technology for monitoring of NOES laminate quality.

Acknowledgments This research was supported by General Motors (GM) and Collaborative Research and Development Grant from Natural Sciences and Engineering Research Council of Canada (NSERC-CRD).

Open Access This article is distributed under the terms of the Creative Commons Attribution License which permits any use, distribution, and reproduction in any medium, provided the original author(s) and the source are credited.

References

- Moses, A.J.: Energy efficient electrical steels: magnetic performance prediction and optimization. *Scr. Mater.* **67**(6), 560–565 (2012)
- Shiozaki, M., Kurosaki, Y.: The effects of grain size on the magnetic properties of nonoriented electrical steel sheets. *J. Mater. Eng.* **11**(1), 37–43 (1989)
- Stephenson, E.T., Marder, A.R.: The effects of grain size on the core loss and permeability of motor lamination steel. *IEEE Trans. Magn.* **22**(2), 101–106 (1986)
- Gutfleisch, O., Willard, M.A., Brück, E., Chen, C.H., Sankar, S.G., Liu, J.P.: Magnetic materials and devices for the 21st century: stronger, lighter, and more energy efficient. *Adv. Mater.* **23**(7), 821–842 (2011)
- Moses A.J.: Possible future trends and research challenges related to 1 & 2 d magnetic properties of soft magnetic materials. *Przepl. Elektr.*, pp. 11–16, (2011)
- Zemánek, I., Havlíček, V.: Universal control and measuring system for modern classic and amorphous magnetic materials single/online strip testers. *J. Magn. Magn. Mater.* **304**(2), e577–e579 (2006)
- Marketos, P., Zurek, S., Moses, A.J.: Calculation of the mean path length of the Epstein frame under non-sinusoidal excitations using the double Epstein method. *J. Magn. Magn. Mater.* **320**(20), 2542–2545 (2008)
- Tumanski, S.: *Handbook of Magnetic Measurements*. CRC Press, Boca Raton (2011)
- Zirka, S.E., Moroz, Y.I., Marketos, P., Moses, A.J.: Loss separation in nonoriented electrical steels. *IEEE Trans. Magn.* **46**(2), 286–289 (2010)
- Graham Jr, C.D.: Physical origin of losses in conducting ferromagnetic materials. *J. Appl. Phys.* **53**(11), 8276–8280 (1982)
- Bertotti, G.: General properties of power losses in soft ferromagnetic materials. *IEEE Trans. Magn.* **24**(1), 621–630 (1988)
- Jiles, D.C.: Dynamics of domain magnetization and the Barkhausen effect. *Czechoslov. J. Phys.* **50**(8), 893–924 (2000)
- Alessandro, B., Beatrice, C., Bertotti, G., Montorsi, A.: Phenomenology and interpretation of the Barkhausen effect in ferromagnetic materials. *J. Appl. Phys.* **64**(10), 5355–5360 (1988)
- Rautioaho, R., Karjalainen, P., Moilanen, M.: Coercivity and power spectrum of Barkhausen noise in structural steels. *J. Magn. Magn. Mater.* **61**(1), 183–192 (1986)
- Bertotti, G., Fiorillo, F., Sassi, M.P.: Barkhausen noise and domain structure dynamics in Si–Fe at different points of the magnetization curve. *J. Magn. Magn. Mater.* **23**(2), 136–148 (1981)
- Ranjan, R., Jiles, D.C., Rastogi, P.: Magnetic properties of decarburized steels: an investigation of the effects of grain size and carbon content. *IEEE Trans. Magn.* **23**(3), 1869–1876 (1987)
- Yamaura, S., Furuya, Y., Watanabe, T.: The effect of grain boundary microstructure on Barkhausen noise in ferromagnetic materials. *Acta Mater.* **49**(15), 3019–3027 (2001)
- Krause, T.W., Szpunar, J.A., Atherton, D.L.: Anisotropic flux density dependence of magnetic Barkhausen noise in oriented 3 % Si–Fe steel laminates. *IEEE Trans. Magn.* **39**(1), 562–566 (2003)
- Clapham, L., Heald, C., Krause, T.W., Atherton, D.L., Clark, P.: Origin of a magnetic easy axis in pipeline steel. *J. Appl. Phys.* **86**(3), 1574–1580 (1999)
- Iordache, V.E., Hug, E., Buiron, N.: Magnetic behaviour versus tensile deformation mechanisms in a non-oriented Fe-(3 wt%) Si steel. *Mater. Sci. Eng.: A* **359**(1), 62–74 (2003)
- Williams, H.J., Shockley, W., Kittel, C.: Studies of the propagation velocity of a ferromagnetic domain boundary. *Phys. Rev.* **80**(6), 1090 (1950)
- Krause, T.W., Szpunar, J.A., Birsan, M., Atherton, D.L.: Correlation of magnetic Barkhausen noise with core loss in oriented 3 % Si–Fe steel laminates. *J. Appl. Phys.* **79**(6), 3156–3167 (1996)
- Birsan, M., Szpunar, J.A., Krause, T.W., Atherton, D.L.: Correlation between the Barkhausen noise power and the total power losses in 3 % Si–Fe. *J. Appl. Phys.* **79**(8), 6042–6044 (1996)
- Stupakov, O.: Local non-contact evaluation of the AC magnetic hysteresis parameters of electrical steels by the Barkhausen noise technique. *J. Nondestruct. Eval.* **32**(4), 405–412 (2013)
- White, S., Krause, T.W., Clapham, L.: A multichannel magnetic flux controller for periodic magnetizing conditions. *IEEE Trans. Instrum. Meas.* **61**(7), 1896–1907 (2012)
- White, S., Krause, T.W., Clapham, L.: Control of flux in magnetic circuits for Barkhausen noise measurements. *Meas. Sci. Technol.* **18**(11), 3501 (2007)
- Patel, H.V., Zurek, S., Meydan, T., Jiles, D.C., Li, L.: A new adaptive automated feedback system for Barkhausen signal measurement. *Sensors Actuators A* **129**(1), 112–117 (2006)
- White S.: A Barkhausen noise NDE system for CANDU® feeder pipes. Queen’s University (2009)
- ASTM Standard. E112, 2010, standard test methods for determining average grain size ASTM International, West Conshohocken, 2010, doi:10.1520/e0112-10
- Yonamine, T., Landgraf, F.J.G.: Correlation between magnetic properties and crystallographic texture of silicon steel. *J. Magn. Magn. Mater.* **272**, E565–E566 (2004)
- Sakamoto, H., Okada, M., Homma, M.: Theoretical analysis of Barkhausen noise in carbon steels. *IEEE Trans. Magn.* **23**(5), 2236–2238 (1987)
- Krause, T.W., Clapham, L., Atherton, D.L.: Characterization of the magnetic easy axis in pipeline steel using magnetic Barkhausen noise. *J. Appl. Phys.* **75**(12), 7983–7988 (1994)
- Matsumura, K., Fukuda, B.: Recent developments of non-oriented electrical steel sheets. *IEEE Trans. Magn.* **20**(5), 1533–1538 (1984)
- Cullity, B.D., Graham, C.D.: *Introduction to Magnetic Materials*. Wiley, Hoboken (2011)
- Chikazumi, S., Charap, S.H.: *Physics of Magnetism*. Wiley, New York (1964)
- Carr Jr, W.J.: Energy loss resulting from domain wall motion. *J. Appl. Phys.* **30**(4), S90–S91 (1959)